CrossMark

ORIGINAL

Heat transfer and pressure drop characteristics of the tube bank fin heat exchanger with fin punched with flow redistributors and curved triangular vortex generators

Song Liu[1,2] · Hua Jin[1,2] · KeWei Song[1,2] · LiangChen Wang[2,3] · Xiang Wu[1,2] · LiangBi Wang[1,2]

Abstract The heat transfer performance of the tube bank fin heat exchanger is limited by the air-side thermal resistance. Thus, enhancing the air-side heat transfer is an effective method to improve the performance of the heat exchanger. A new fin pattern with flow redistributors and curved triangular vortex generators is experimentally studied in this paper. The effects of the flow redistributors located in front of the tube stagnation point and the curved vortex generators located around the tube on the characteristics of heat transfer and pressure drop are discussed in detail. A performance comparison is also carried out between the fins with and without flow redistributors. The experimental results show that the flow redistributors stamped out from the fin in front of the tube stagnation points can decrease the friction factor at the cost of decreasing the heat transfer performance. Whether the combination of the flow redistributors and the curved vortex generators will present a better heat transfer performance depends on the size of the curved vortex generators. As for the studied two sizes of vortex generators, the heat transfer performance is promoted by the flow redistributors for the fin with larger size of vortex generators and the performance is suppressed by the flow redistributors for the fin with smaller vortex generators.

List of symbols

A Heat transfer area (m^2)
A_a Total air-side surface area (m^2)
A_e Heat transfer area of the flow domain formed by two adjacent fins (m^2)
A_f Fin surface area in contact with air (m^2)
A_t Tube surface area in contact with air (m^2)
A_w Inside surface area of the tube (m^2)
c_p Specific heat at constant pressure (J kg^{-1} K^{-1})
D_e Hydraulic diameter (m)
D_i Inner diameter of the tube (m)
D_o Outer diameter of the tube (m)
f Friction factor
F_T Correction factor of logarithmic-mean temperature difference
h Heat transfer coefficient (W m^{-2} K^{-1})
H Height of curved vortex generators (m)
L Base length of curved vortex generators (m)
L_f Length of fin along flow direction (m)
m Mass flow rate (kg s^{-1})
Nu Nusselt number
p Pressure (Pa)
Pr Prandtl number
Q Heat transfer rate (W)
r_c Outside radius of fin collar (m)
Re Reynolds number
S_1 Transversal distance of tubes (m)
S_2 Longitudinal distance of tubes (m)
t Temperature (°C)
T Temperature (K)
T_p Fin spacing (m)
u Velocity (m s^{-1})

✉ LiangBi Wang
lbwang@mail.lzjtu.cn

1   School of Mechanical Engineering, Lanzhou Jiaotong University, Lanzhou 730070, Gansu, People's Republic of China

2   Key Laboratory of Railway Vehicle Thermal Engineering of MOE, School of Mechanical Engineering, Lanzhou Jiaotong University, Lanzhou 730070, Gansu, People's Republic of China

3   School of Chemistry and Chemical Engineering Science, Lanzhou Jiaotong University, Lanzhou 730070, Gansu, People's Republic of China

🙋 Springer

U	Overall heat transfer coefficient (W m^{-2} K^{-1})
V_e	Volume of the flow domain formed by two adjacent fins (m^3)

Greeks

k	Thermal conductivity (W m^{-1} K^{-1})
η	Fin efficiency
η_o	Overall fin efficiency
μ	Dynamic viscosity (kg m^{-1} s^{-1})
ρ	Density (kg m^{-3})
δ	Fin thickness (m)
Δp	Pressure drop (Pa)
Δt	Temperature difference (K)
ΔT_m	Logarithmic-mean temperature difference

Subscripts

a	Air-side
f	Fin
in	Inlet
m	Mean value
max	Maximum value
out	Outlet
t	Tube
w	Water

1 Introduction

Heat exchangers are widely used in many industrial systems, such as air conditioning condensers and evaporators, machine cooling, chemical processes, aerospace and so on. The development trends of these heat exchangers are to improve the heat transfer efficiency and reduce energy consumption. But the heat transfer performance is limited by the air-side thermal resistance in such heat exchangers. Thus, enhancing the air-side heat transfer is an effective method to improve the performance of the heat exchanger. Many fin patterns including wavy fin [1], slit fin [2], louvered fin [3], fin with vortex generators (VGs) [4] and some combination of enhanced fins [5, 6] are investigated and widely used. As the air-side heat transfer performance is usually affected by many parameters, until today these fin patterns with different parameters and novel techniques continue to draw the attention of researchers.

Tang et al. [7–9] studied the air-side friction and heat transfer characteristics of the fin-and-tube heat exchangers with various fin patterns: crimped plain fin, spiral fin, slit fin, fin with delta-wing longitudinal vortex generators and mixed fin for which the number of tube rows was 12 and the diameter of the tubes was 18 mm over all numerical and experimental investigations. Zeng et al. [10] numerically studied the influence of various design parameters on the heat transfer and friction factor characteristics of

fins with vortex generators. The results indicated that the intensity of heat transfer was greatly increased with the increase of attack angle, length and height of vortex generators, accompanied with an increase in pressure drop. Wu and Tao [11] carried out a research about the parameters of longitudinal vortex generators. Their findings indicated that the attack angle of 45° provided the best heat transfer enhancement. Song et al. [12] studied the heat transfer enhancement of fins by mounting vortex generators on both surfaces of the fin and reported an optimum arrangement of vortex generators for best heat transfer performance. Gao et al. [13] studied the optimum height of winglet vortex generators mounted on three-row flat tube bank fin. The optimum height of VGs is dependent on the thickness of the fin and its thermal conductivity. For mostly used fin thickness and material, the optimum height of VGs is 0.8 times as large as the net fin spacing. Liu et al. [14] experimentally studied the effect of transversal tube pitch on heat transfer characteristics of heat exchangers with VGs. The results indicated that the heat transfer coefficient increases with increasing the transversal tube pitch. Song et al. [15] numerically studied the effect of the transversal pitch of vortex generators on heat transfer and interaction of vortices. An optimum transversal pitch for best heat transfer performance and an undesired transverse pitch that should be avoided were reported. Zhang et al. [16] experimentally investigated the span position of VGs of three-row flat tube bank fin heat exchangers and found that VGs should be mounted as close as possible to the tube wall. Hu et al. [17] numerically studied the effect of fin spacing of circle tube bank fin heat exchangers with vortex generators on the thermal–hydrodynamic performance. Optimum fin spacing for the circle tube bank fin heat exchanger with vortex generators was reported.

Besides the fin and vortex generator parameters, the type of vortex generators has received wide attention. Jang et al. [18] numerically observed the thermal hydraulic characteristics of a 3-D laminar inline and staggered plate and tube heat exchanger with block-type vortex generators mounted behind the tubes. Optimization of the span angle and location of vortex generators was investigated by a simplified conjugate-gradient method. The results showed that the best heat transfer performance can be obtained when the span angle of VG ranges from 30° to 60° and the transversal location of VG ranges from 2 to 20 mm. Song et al. [19] experimentally studied the effect of curved delta winglet vortex generators on fluid flow and heat transfer characteristics of circular tube bank fin heat exchangers. They reported that the curved vortex generator can effectively enhance the heat transfer performance of the fin. Larger size of curved vortex generators is beneficial to the heat transfer enhancement for flow with large *Re,* while the smaller curved vortex generator is advantageous to heat

transfer enhancement for flow with low *Re*. They also reported that the change of fin pitch has less effect on Colburn factor but obviously affects the friction factor. Lotfi et al. [20] investigated thermal hydraulic characteristics of a new smooth wavy fin-and-elliptical tube heat exchanger with three new types of VGs. In their study, the influence of the geometric shape of the VGs, attack angle of the winglet VGs, tube ellipticity ratio and wavy fin height on the thermal hydraulic performance of three new types of VGs was investigated. Colleoni et al. [21] investigated the optimum configuration of heat exchanger with VGs combined with riblets. The results indicated that when the height of VGs is half of the channel height, the longer and thinner riblets have better thermal performance. Zhou et al. [22] carried out an experimental study about heat transfer enhancement by plane and curved winglet-type vortex generators with punched holes. They found that the punched holes really improved the thermal hydraulic performance of VGs.

From the above mentioned researches we can find that the air-side heat transfer and pressure drop characteristics are widely studied and the performance has been improved. The optimization of the fin and vortex generator parameters is the main object. As we know that there are stagnation points and wake regions behind the circular tubes, which lead to remarkable increasing of pressure drop around the stagnation points of tubes and decreasing of heat transfer in wake regions. An effective approach to overcome the disadvantages of this type of heat exchanger is to improve the flow field structure through variation of fin surface geometry. In this paper, a new fin pattern with flow redistributors and curved triangular vortex generators (CTVG) is reported. The effects of flow redistributors, curved triangular vortex generators and the combination of flow redistributors and curved triangular vortex generators on heat transfer and pressure drop characteristics are experimentally studied.

2 Experimental apparatus

The performance test of the studied heat exchanger is carried out on the special experimental platform, as shown in Fig. 1. The experimental platform consists of a semi-open low-speed wind tunnel and a water circulation system. The wind tunnel mainly consists of an electromotor, a centrifugal fan, expansion section, transition section, test section, straight section, rectifying section and contraction section. The centrifugal fan is controlled by a variable frequency electromotor with a rated power of 5.5 kW to achieve the purpose of variable flow rate. A frequency converter is used to supply the current with frequency changing between 0.01 and 50 Hz. The accurate air flow rate which is tested by Pitot tube installed in the test section can be adjusted by the butterfly valve installed at the outlet of the centrifugal fan. The inlet air temperature of the test section is adjusted by altering the ratio of the cold air from the inlet of the tunnel to the hot air from the outlet of the centrifugal fan using the butterfly valves which are installed at the inlet and the Y-shaped branch of the wind tunnel. The water circulation system includes a water pump, a water heating tank and the related circulating pipes. The rated power of the heating tank is 90 kW. The water is heated to a certain temperature by several electric heating tubes in the water tank before being pumped to the heat exchanger. The flow rate of the water is controlled by a variable frequency pump. A turbine flow meter is used to measure the accurate flow rate.
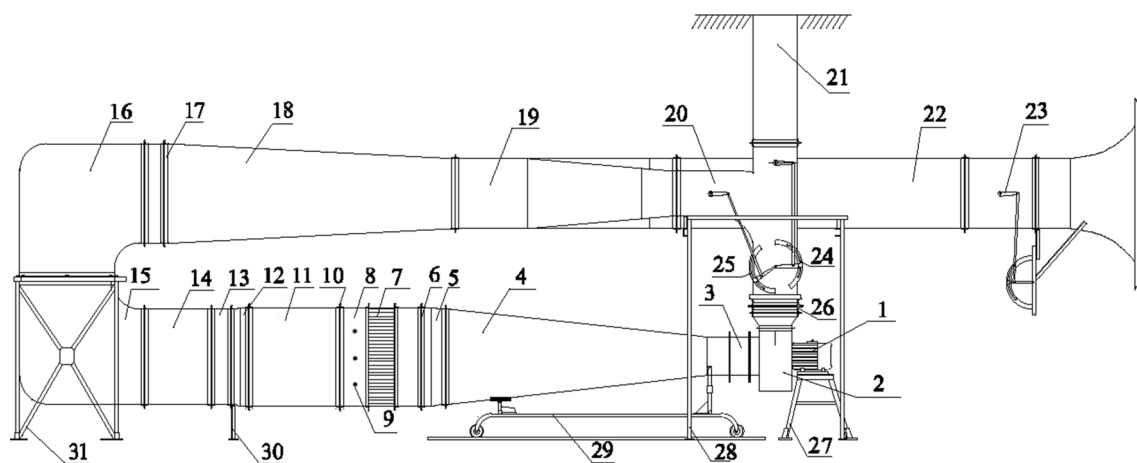
Fig. 1 Schematic view of the experimental platform. *1* Electromotor, *2* centrifugal fan, *3* soft tube, *4* contraction section, *5* transition section, *6* thermal resistance net, *7* heat exchanger, *8* test section, *9* Pitot tube, *10* thermal resistance net, *11* straight section, *12* transition section, *13* rectifying net, *14* rectifying section, *15–16* turning, *17* rectifying net, *18* expansion duct, *19* joint body, *20* Y-shaped branch, *21* outlet, *22* inlet, *23–25* butterfly valves, *26* outlet of centrifugal fan, *27–31* supporting frame

Figure 2 shows the schematic view of the test section. The heat exchanger is installed inside the section with the cross section of the heat exchanger being equal to the cross section of the test section. The outside of the test section is insulated with thermal insulation material. The copper thermal resistance nets which are used to measure the inlet and outlet temperature of the air through the heat exchanger are installed at both ends of the test section. The static pressure is measured through the static poles around the straight section using the U-shaped mercury manometer. The pressure drop of air flowing through the heat exchanger is measured using an inclined manometer. The differential pressure of the Pitot tube is measured by compensated micro-pressure meter. The Pitot tube measures the local velocity at the measuring point in the flow field, but if the Pitot tube is located at the position where the velocity is just the mean velocity of the cross section, and the local velocity is multiplied by the area of the cross section where the Pitot tube is located, the total volume flow rate can be obtained. Then the mass flow rate of air can be obtained on the measured cross section. Thus, it is very important to find the corrected positions where the Pitot tubes are located. In the process
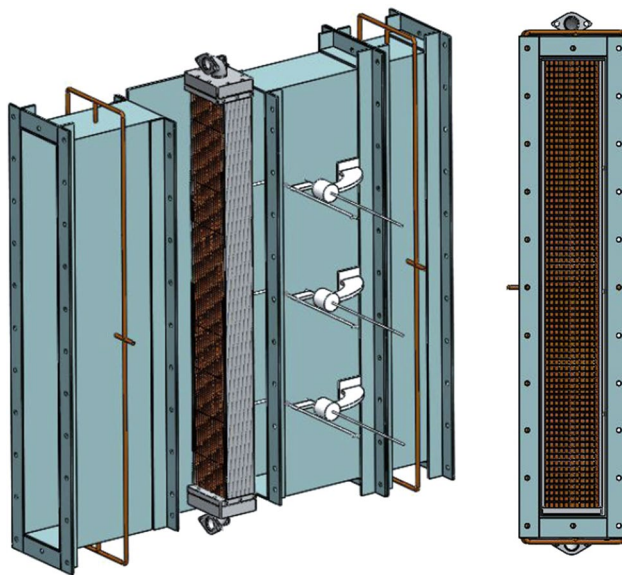
of adjusting the experimental set up, these locations are carefully calibrated many times at different volume flow rates. The average inlet velocity through the cross-sectional area just at the entrance of the heat exchanger and the maximum mean velocity through the minimum cross-sectional flow area of the heat exchanger are calculated from the mass conservation law. In this process, the air density is calculated by the gas state equation using the average air temperature of the inlet and the outlet temperatures, and the average static pressure of the inlet and the outlet static pressures. The temperature of the water is measured in the temperature-measure tanks at the inlet and outlet of the heat exchanger using the mercury thermometers with a minimum resolution of 0.1 °C.
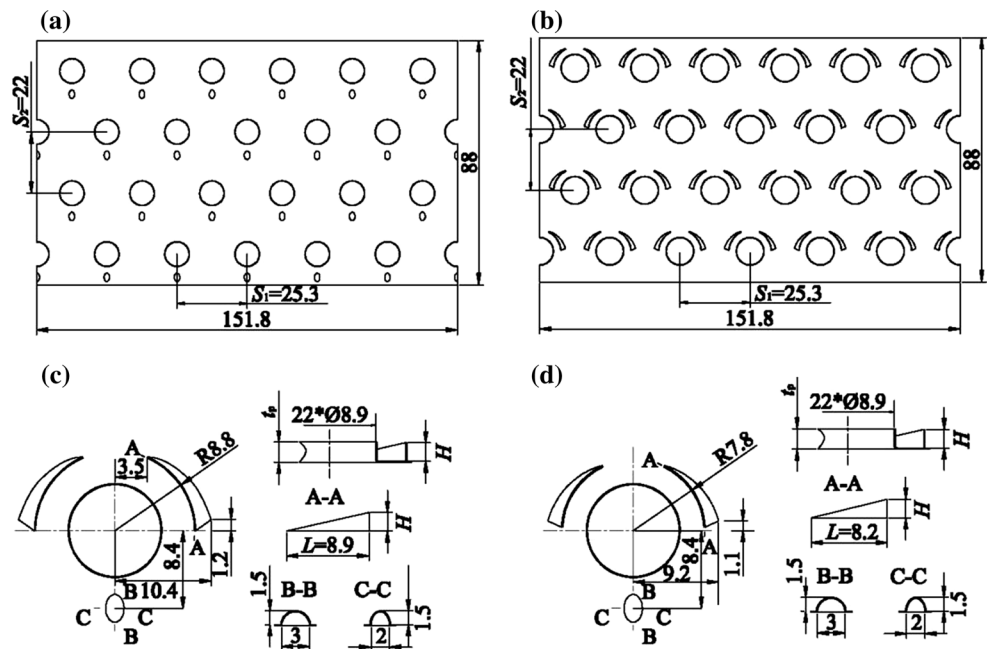
In the process of the experiment, circulating water was heated to 90 °C and cooled by the air of 40 °C inside the heat exchanger. The flow rate of water is 2 ms^{-1}. The inlet water temperature and the inlet air temperature were fixed. Only the velocity of air was adjusted within a certain range. All the experimental data was recorded when the system reached a state of thermal equilibrium and the heat balance error was less than 5%. Each of the test points must be recorded at least 6 times to avoid abnormal error and reduce random error.

The real heat exchanger studied in this paper is designed for the diesel locomotives used in China. Figure 3a shows the schematic view of the heat exchanger with semi-ellipsoidal flow redistributors stamped out from the plain fins. Figure 3b shows the schematic view of the studied heat exchanger with curved triangular vortex generators and semi-ellipsoidal flow redistributors. The curved triangular vortex generators are arranged around the tube and the semi-ellipsoidal flow redistributors are located in front of the stagnation point of each tube. Figure 3c shows the schematic view of the flow around one tube together with a flow redistributor and CTVGs. The flow redistributors are protrusions that stamped out using a stamping forming process. On the opposite side of the protrusions, there are dimples on the fin surface. The height of the flow redistributors is 1.5 mm. The major axis of the base ellipse is 3.0 mm and the minor axis is 2.0 mm. Cold air flows through the channel formed by tubes and fins, and hot water flows in the tubes. All the tested heat exchangers are new specimen

Fig. 2 Schematic view of the test section

Fig. 3 Schematic view of the studied heat exchanger, a fin with flow redistributors, b fin with flow redistributors and CTVGs, c flow around CTVGs and redistributors
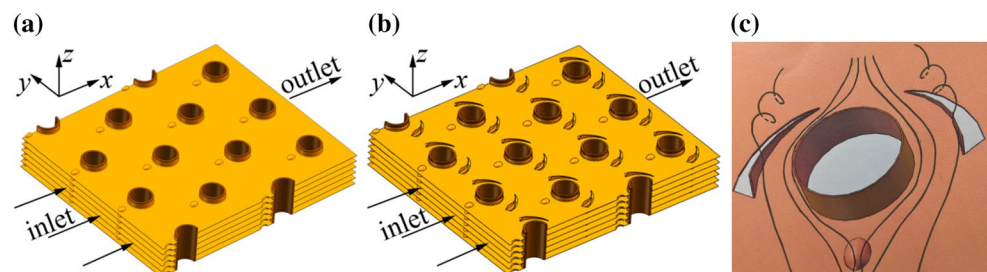
Fig. 4 Fin configuration: **a** plain fin with flow redistributors; **b** fin with CTVG; **c** CTVG-I; **d** CTVG-II

specially made for the experiment and are flushed before the installation in the test section of the wind tunnel. The circulating water system is clean and the fouling effect inside the tube is not considered. The dimensions of the heat exchanger are 1127 mm × 151.8 mm × 88 mm. Three fin pitches, T_p = 1.7, 2.0 and 2.3 mm are studied in this paper. The thickness of the fin is 0.12 mm. There are 663, 563, 490 pieces of fins for the fin pitches T_p = 1.7, 2.0 and 2.3 mm, respectively. There are a total of 22 tubes with a staggered tube arrangement. The outer diameter of tube is 8.9 mm and the inner diameter is 8.0 mm. The total inner surface area of the tubes is 0.623 m². The total outer surface areas of the tubes contacting with the air are A_t = 0.680, 0.689 and 0.694 m² for T_p = 1.7, 2.0 and 2.3 mm, respectively. The total surface areas of the fins in contact with the air are A_f = 15.505, 12.909 and 11.412 m² for T_p = 1.7, 2.0 and 2.3 mm, respectively.

Figure 4 shows the geometrical configuration of the fins, vortex generators and flow redistributors. Two sizes of curved triangular vortex generators are studied. The base length of one of the curved triangular vortex generator (CTVG-I) is L = 8.9 mm and the other one (CTVG-II) is L = 8.2 mm. Both the tubes and fins are made of copper. The transversal tube pitch S_1 is 25.3 mm. The longitudinal tube pitch S_2 is 22 mm. The base circle radius of CTVG-I is 8.8 mm, and the base circle radius of CTVG-II is 7.8 mm. The center of the base circles of CTVG-I and CTVG-II coincides with the center of the tube. The plain fin and the plain fin with flow redistributors are also studied for comparison. There are a total of 18 fin patterns studied in this paper. The detailed parameters of the fin patterns are shown in Table 1.

3 Data reduction

The heat transfer characteristic of the heat exchanger is determined using the data recorded at a steady state condition. The total heat transfer rates from air-side and water-side are averaged as follows:

$$Q_a = m_a c_{p,a} \Delta t_a \tag{1}$$

Table 1 Parameters of fin and CTVG

No.	Fin type	T_p (mm)	L (mm)
1	Plain fin	1.7	–
2	Plain fin	2.0	–
3	Plain fin	2.3	–
4	Plain fin with flow redistributors	1.7	–
5	Plain fin with flow redistributors	2.0	–
6	Plain fin with flow redistributors	2.3	–
7	CTVG-I	1.7	8.9
8	CTVG-I	2.0	8.9
9	CTVG-I	2.3	8.9
10	CTVG-II	1.7	8.2
11	CTVG-II	2.0	8.2
12	CTVG-II	2.3	8.2
13	CTVG-I and flow redistributors	1.7	8.9
14	CTVG-I and flow redistributors	2.0	8.9
15	CTVG-I and flow redistributors	2.3	8.9
16	CTVG-II and flow redistributors	1.7	8.2
17	CTVG-II and flow redistributors	2.0	8.2
18	CTVG-II and flow redistributors	2.3	8.2

$$Q_{\mathrm{w}} = m_{\mathrm{w}} c_{\mathrm{p,w}} \Delta t_{\mathrm{w}} \tag{2}$$

$$Q_m = (Q_a + Q_{\mathrm{w}})/2 \tag{3}$$

The overall heat transfer coefficient, U, is calculated from the following relationship:

$$UA = Q_{\mathrm{m}} \big/ (F_{\mathrm{T}} \Delta T_{\mathrm{m}}) \tag{4}$$

The logarithmic-mean temperature difference, ΔT_{m}, is defined by

$$\Delta T_{\mathrm{m}} = \frac{\left(T_{\mathrm{w,in}} - T_{\mathrm{a,out}}\right) - \left(T_{\mathrm{w,out}} - T_{\mathrm{a,in}}\right)}{\ln\left(\left(T_{\mathrm{w,in}} - T_{\mathrm{a,out}}\right) \big/ \left(T_{\mathrm{w,out}} - T_{\mathrm{a,in}}\right)\right)} \tag{5}$$

The correction factor of logarithmic-mean temperature difference, F_{T} is [23]:

$$F_T = \frac{\ln(\frac{1-P}{1-RP})}{(1-R)\ln[1 + \frac{1}{R}\ln(1 - RP)]} \tag{6}$$

$$R = \frac{T_{\mathrm{a,out}} - T_{\mathrm{a,in}}}{T_{\mathrm{w,in}} - T_{\mathrm{w,out}}}, \quad P = \frac{T_{\mathrm{w,in}} - T_{\mathrm{w,out}}}{T_{\mathrm{w,in}} - T_{\mathrm{a,in}}} \tag{7}$$

The overall heat transfer resistance can be defined as:

$$\frac{1}{UA} = \frac{1}{\eta_0 h_a A_a} + \frac{1}{2}\ln\frac{D_0}{D_i}\frac{D_0}{k_t A_t} + \frac{1}{h_{\mathrm{w}} A_{\mathrm{w}}} \tag{8}$$

h_w is predicted using the equation reported in [24]:

$$h_{\mathrm{w}} = 1057 C_f (1.352 + 0.02t)\left(\frac{u^{0.8}}{D_i^{0.2}}\right) \tag{9}$$

$$C_f = -0.1864 \ln(D_i) + 0.22455 \tag{10}$$

C_f is the correction factor related to the inner diameter of the tube.

The overall surface efficiency, η_o, is defined as the ratio of actual heat transfer rate of the fin to the heat transfer rate of the fin at the same temperature as the fin base. This term may be written in terms of the fin efficiency η, fin surface area A_{f} and total air-side area A_{a} as follows:

$$\eta_0 = 1 - \frac{A_{\mathrm{f}}}{A_{\mathrm{a}}}(1 - \eta) \tag{11}$$

$$A_{\mathrm{a}} = A_{\mathrm{t}} + A_{\mathrm{f}} \tag{12}$$

A_{t} and A_{f} are the areas of the tube and fin surfaces that are in contact with the air. η denotes the fin efficiency and is calculated by the approximation method described by Schmidt [25]:

$$\eta = \frac{\tanh(mr_c\phi)}{mr_c\phi} \tag{13}$$

$$m = \sqrt{\frac{2h_{\mathrm{a}}}{k\delta}} \tag{14}$$

$$\phi = (R_{eq}/r_c - 1)[1 + 0.35\ln(R_{eq}/r_c)] \tag{15}$$

$$R_{eq}/r_c = 1.27(X_{\mathrm{M}}/r_c)(X_{\mathrm{L}}/X_{\mathrm{M}} - 0.3)^{1/3} \tag{16}$$

$$X_{\mathrm{L}} = \left(\sqrt{(S_1/2)^2 + (S_2)^2}\right)/2 \tag{17}$$

$$X_{\mathrm{M}} = S_1/2 \tag{18}$$

The air-side heat transfer coefficient h_{a} and the surface efficiency η_{o} can be acquired through solving Eqs. (8)–(18) with an iterative method [9].

The air-side hydraulic diameter is defined as:

$$D_{\mathrm{e}} = \frac{4V_{\mathrm{e}}}{A_{\mathrm{e}}} \tag{19}$$

V_{e} is the flow domain formed by two adjacent fins of the heat exchanger, and A_{e} is the corresponding heat transfer area of the flow domain. For a minimum flow unit, V_{e} is equal to the product of a single-side area of the fin surface and the fin space, and A_{e} is equal to the sum of the area of fin and tube surfaces that contact with air.

$$V_{\mathrm{e}} = \left(4S_2 \times \frac{S_1}{2} - 4 \times \frac{1}{2}\frac{\pi D_{\mathrm{o}}^2}{4}\right) \times (T_{\mathrm{p}} - \delta) \tag{20}$$

$$A_{\mathrm{e}} = \left(4S_2 \times \frac{S_1}{2} - 4 \times \frac{1}{2}\frac{\pi D_{\mathrm{o}}^2}{4}\right) \times 2 + 4 \times \frac{1}{2}\pi D_{\mathrm{o}}(T_{\mathrm{p}} - \delta) \tag{21}$$

The Reynolds number of the air-side is defined as:

$$Re = \frac{\rho_{\mathrm{a}} u_{\mathrm{max}} D_{\mathrm{e}}}{\mu_{\mathrm{a}}} \tag{22}$$

The average Nusselt number of the air-side is defined as:

$$Nu = \frac{h_{\mathrm{a}} D_{\mathrm{e}}}{k_{\mathrm{a}}} \tag{23}$$

The friction factor of the air is defined as:

$$f = \frac{2\Delta p}{\rho_{\mathrm{a}} u_{\mathrm{max}}^2}\frac{D_{\mathrm{e}}}{L_{\mathrm{f}}} \tag{24}$$

To verify the validity of the experiment system used in this study, the air-side performance experiment of the heat exchanger with traditional plain fin is also conducted. The experimental results of Nu for the plain fin with 4 tube rows are compared with the well-known correlation of Gray [26], and the experimental results of f are compared with the well-known correlation of Wang

[27], as shown in Fig. 5. The hydraulic diameter is defined using the outer tube diameter. The maximum difference in *Nu* between the present data and the correlation is 8.65% when *Re* is about 11,757, and the minimum difference in *Nu* is 0.46% when *Re* is about 6000. The maximum difference in *f* between the present data and the well-known correlation of Wang [27] is 11.0% when *Re* is about 3290, and the minimum difference in *f* is 2.0% when *Re* is about 7400. For the performance experiments of the heat exchanger, the uncertainty of *Nu* is 6.9% and the uncertainty of *f* is 8.1% according to the single sample theory of Moffat [28]. Thus, the present experiment system is reliable.

4 Experimental result and discussions

4.1 Effects of flow redistributors on *Nu* and *f* of plain fin

The distributions of *Nu* for plain fin and the fin with flow redistributors under different fin pitches are shown in Fig. 6a. *Nu* increases with the increase of both *Re* and T_p for both fin patterns. The distributions of *Nu* are obviously affected by the flow redistributors. There is an obvious difference in *Nu* between plain fins with and without flow redistributors. When the flow redistributors are stamped out from the fin surface in front of the stagnation points of


Fig. 5 Verification of experimental results with correlations: **a** *Nu*; **b** *f*
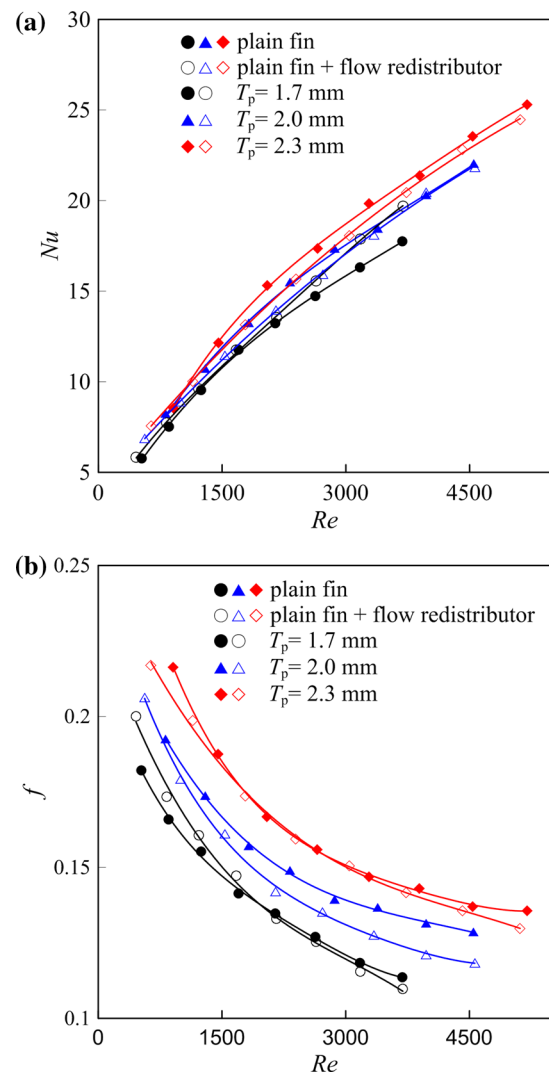
Fig. 6 Comparison of *Nu* and *f* between plain fin and the fin with flow redistributors: **a** *Nu*; **b** *f*

the tubes, the air changes direction and flows around the flow redistributors as shown in Fig. 3c. Flow disturbance is caused by the flow redistributors. The local heat transfer is undoubtedly enhanced in the region where flow redistributors locate. Meanwhile, the flow velocity behind the flow redistributors decreases and the heat transfer decreases both in the region behind the flow distributors and near the stagnation position of the tube. When the fin pitch is 1.7 mm which is a little larger than the height of flow redistributors, there is a narrow slit between the fin and the flow redistributors and the jet effect from the slit is good for heat transfer. The flow redistributors cause an obvious effect on heat transfer especially when Re is larger than 2000. The heat transfer enhancement due to flow redistributors is larger than the decrease of heat transfer in the region behind the flow redistributors. Thus, the value of Nu of the fin with flow redistributors is larger than the fin without flow redistributors. When the fin pitch increases to $T_p = 2.0$ and 2.3 mm, the relative height of flow distributors decreases compared with the fin pitch. Both the jet effect through the slit and the effect of flow redistributors on the flow disturbance decrease. Although the existence of flow redistributors can enhance the local heat transfer, the flow redistributors are relatively small compared with the tube area. The decreases of heat transfer in the fin region behind the flow redistributors and on the tube surface are larger than the heat transfer enhancement caused by flow redistributors. Thus, the value of Nu of the fin with flow redistributors is smaller than that of the plain fin without flow redistributors when the fin pitch is greater than 2.0 mm.

Figure 6b shows the comparison of f between plain fin and the fin with flow redistributors. The value of f increases with the increase of fin pitches for both fin patterns. When flow redistributors are stamped out from the fin surface, the air flow direction changes and flows over the flow redistributors. The velocity of the flow in front of the stagnation point of the tube decreases due to the existence of flow redistributors located in front of the tubes, and the pressure drop around the tube also decreases. Therefore the value of f of the plain fin with flow redistributors is generally smaller than that of plain fin when $T_p > 2.0$ mm. The value of f of the plain fin with flow redistributors is larger than that of the plain fin when $T_p = 1.7$ mm and $Re < 2000$ due to the increase of pressure drop in the region where flow redistributors are located. From this figure we can find that the existence of flow redistributors can decrease the value of f at the cost of decreasing the value of Nu.

4.2 Comparison of Nu and f between plain fin and fin with CTVG-II

Figure 7 shows the comparison of Nu and f between plain fin and the fin with CTVG-II. The main purpose
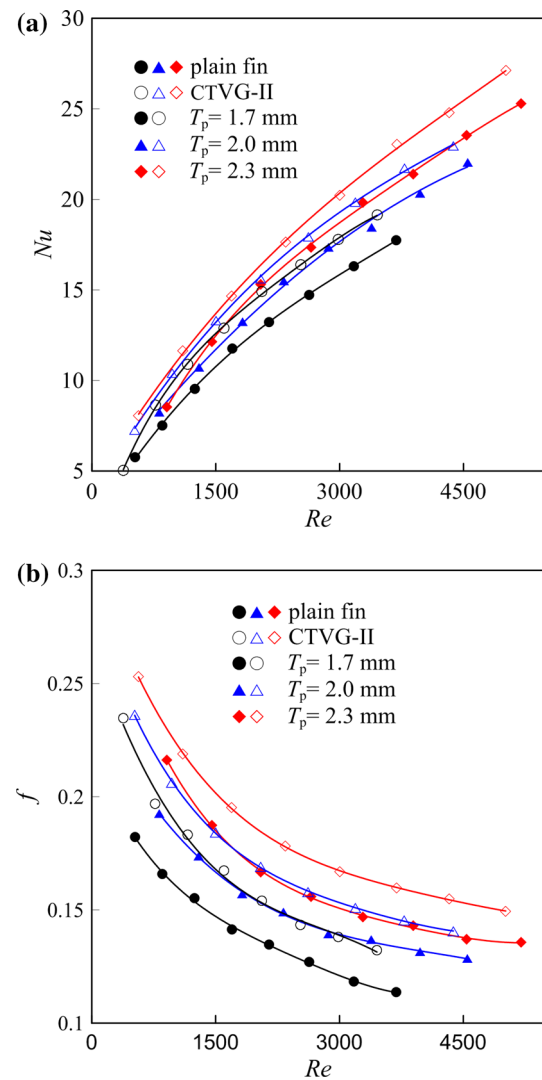
Fig. 7 Comparison of Nu and f between plain fin and fin with CTVG-II: **a** Nu; **b** f

of applying CTVGs around the circle tube is to enhance the heat transfer. The arrangement of CTVG-II around the circle tube can induce the fluid to flow into the wake region and restrain the flow separation. The area of the wake zone behind the circular tube is reduced significantly, hence the heat transfer enhancement and the decrease of pressure loss behind the tube are resulted. It is quite obvious that the value of Nu of the fin with CTVG-II is greatly increased compared with that of the plain fin due to the existence of CTVG-II. Both the value of Nu and the differences in Nu for the fin with different fin pitches increase with the increase in Re. The difference in Nu between the plain fin and the fin with CTVG-II also increases with increasing Re. The value of f decreases along with the increase in Re and increases with the increase of fin pitch for both fin patterns. The

value of f of the fin with CTVG-II is obviously larger than that of the plain fin. From this figure we can find that CTVG-II can enhance heat transfer effectively at the cost of increasing the friction factor.
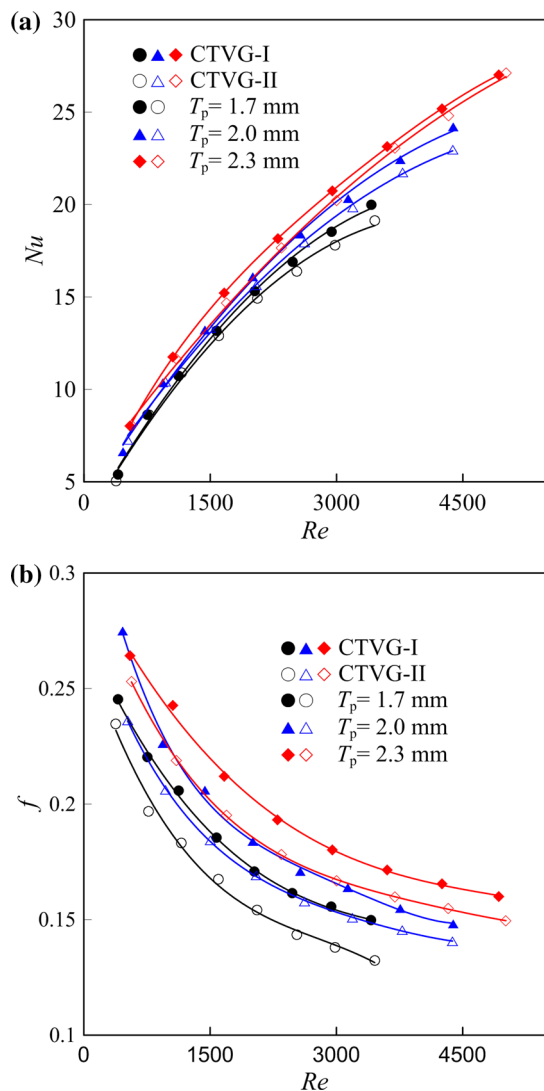
4.3 Comparison of Nu and f between fins with CTVG-I and CTVG-II

Two sizes of CTVGs, CTVG-I and CTVG-II, are studied in this paper. The heights of CTVG-I and CTVG-II are the same. The base length of CTVG-I is longer than that of CTVG-II, as shown in Fig. 4. The comparisons of Nu and f between fins with CTVG-I and CTVG-II are shown in Fig. 8. The distributions of Nu and f are similar to each other for both fin patterns with CTVG-I and CTVG-II. Nu increases with increasing both Re and T_p. As the size

Fig. 8 Comparison of Nu and f between fins with CTVG-I and CTVG-II: **a** Nu; **b** f

of CTVG-I is larger than CTVG-II, CTVG-I can induce more fluid to flow into the wake zone behind the tubes. Meanwhile, CTVG-I can generate a stronger secondary flow which determines the heat transfer intensity in the flow channel of fin-and-tube heat exchangers with vortex generators [29–32]. Thus, the value of Nu of the fin with CTVG-I is larger than that of the fin with CTVG-II for all the studied fin pitches and the difference in Nu increases with the increase of Re. The value of f also increases with the increase of both Re and T_p for both fins with CTVG-I and CTVG-II. The value of f of the fin with CTVG-I is obviously larger than that of the fin with CTVG-II.

4.4 Effect of flow redistributors on Nu and f for fins with CTVG-I and CTVG-II

From Figs. 6, 7, 8 we can find that both CTVG-I and CTVG-II can enhance the heat transfer at the cost of increasing the friction factor, while the flow redistributors can decrease the friction factor at the cost of decreasing heat transfer. Figure 9 shows the distributions of Nu and f for the fin with CTVG-I and the fin with both CTVG-I and flow redistributors. Both Nu and f increase with the increase of fin pitches. The difference in Nu between the fins with and without flow redistributors is small, and the values of Nu are nearly the same when $Re < 2000$. The value of Nu for the fin with CTVG-I and flow redistributors increases compared with that of the fin with only CTVG-I due to the existence of flow redistributors when the fin pitch is greater than 2.0 mm and $Re > 2000$. When the fin pitch is 1.7 mm, the difference in Nu between the fin with CTVG-I and the fin with both CTVG-I and flow redistributors is very small, and the values of Nu are nearly the same. The value of f for the fin with CTVG-I and flow redistributors is generally larger than that of the fin with CTVG-I. The value of f for the fin with CTVG-I and flow redistributors is smaller than that of the fin with CTVG-I when $Re > 2000$ and $T_p = 1.7$ mm. CTVGs are mainly used to restrain the flow separation and induce the fluid to flow into the wake region, while the flow redistributors are used to redistribute the flow in front of the tube. When flow redistributors are stamped out in front of the fin with CTVGs, the flow velocity decreases in front of the tube with a decrease in pressure loss. Meanwhile the velocity increases in the region away from the tube. The fluid with high velocity flows toward the CTVG-I which can induce the fluid to flow into the wake region, hence the decrease of wake zone and heat transfer enhancement. Meanwhile the increase in velocity around CTVG-I causes an increase in pressure loss. The combined result is that the heat transfer increases with a little increase in pressure loss. Flow redistributors can enhance the heat transfer at the cost of increasing pressure loss for the fin with CTVG-I.
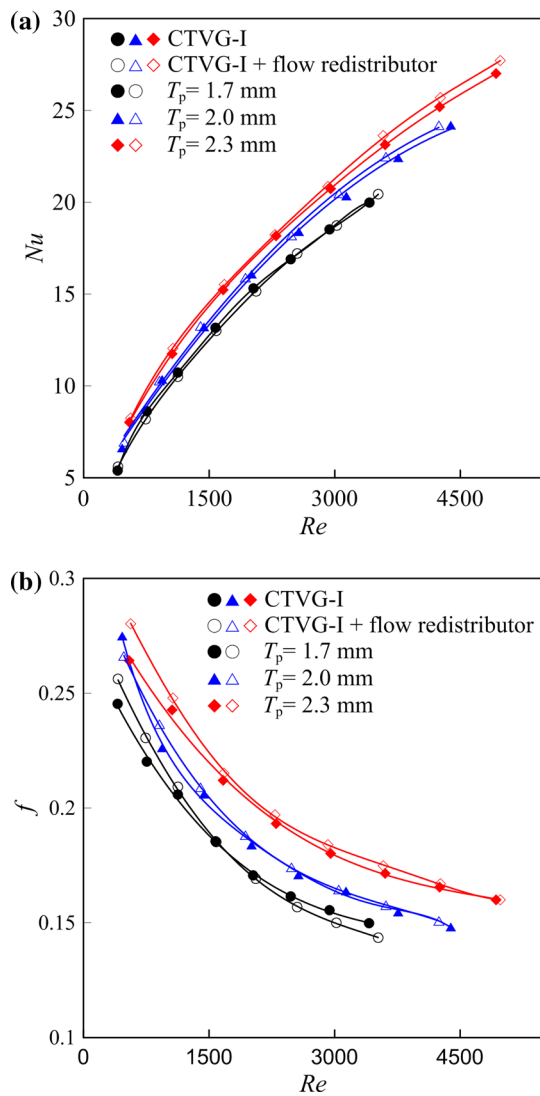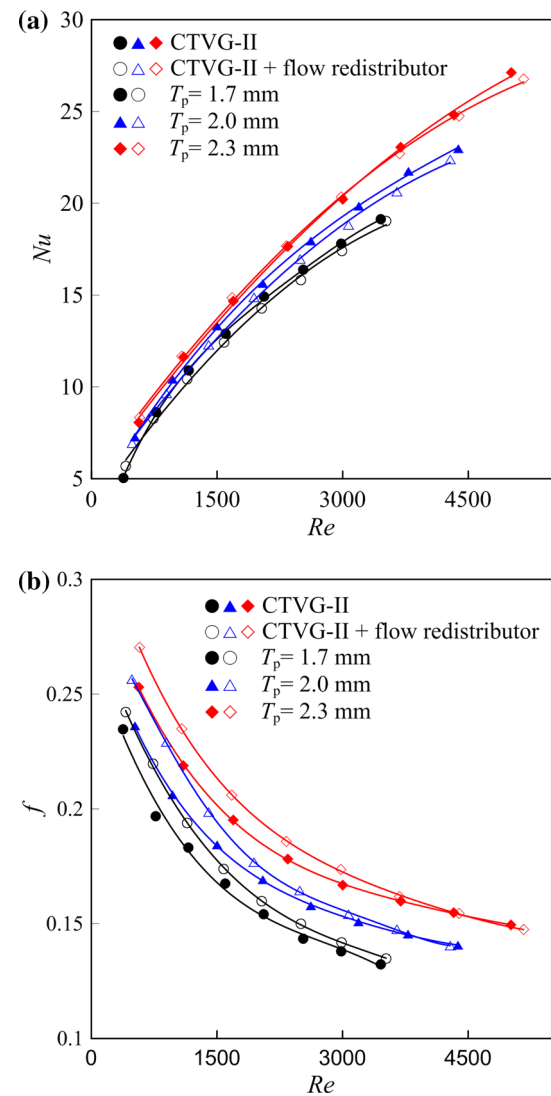
Fig. 9 Effect of flow redistributors on Nu and f for the fin with CTVG-I: **a** Nu; **b** f

**Fig. 10** Effect of flow redistributors on Nu and f for the fin with CTVG-II: **a** Nu; **b** f

Figure 10 shows the distributions of Nu and f for the fin with CTVG-II and the fin with both CTVG-II and flow redistributors. The difference in Nu between different fin pitches increases with the increase in Re for both fin patterns. Nu of the fin with both CTVG-II and flow redistributors is smaller than that of the fin with only CTVG-II due to the existence of flow redistributors for all the studied fin pitches. The differences between the values of Nu for the fins with and without flow redistributors are very small for fin pitch $T_p = 2.3$ mm, the values of Nu are nearly the same when $Re < 4000$. The existence of flow redistributors has a negative effect on heat transfer of the fin with CTVG-II, which is opposite to the effect of flow redistributors on heat transfer of the fin with CTVG-I. The reason of such opposite effect is that the length of CTVG-I is a little larger than CTVG-II, and CTVG-II is located closer to the tube than

CTVG-I. When flow redistributors are stamped out in front of the tube of fin with CTVG-II, the flow velocity increases in the region away from the tube. The flow rate between the tube and CTVG-II decreases and less fluid was induced into the wake zone behind the tube. Thus, the heat transfer is reduced and pressure loss increases. The value of f increases due to the existence of flow redistributors on the fin with CTVG-II. Compared to Fig. 9, the increment of f of the fin with CTVG-II is larger than that of the fin with CTVG-I due to the existence of flow redistributors. From this figure we can find that flow redistributors stamped out from the fin surface in front of the tubes have a negative effect on heat transfer of the fin with CTVG-II by increasing the pressure loss.

The comparisons of Nu and f for fins with CTVG-I and CTVG-II are shown in Fig. 11. Nu and the difference in Nu
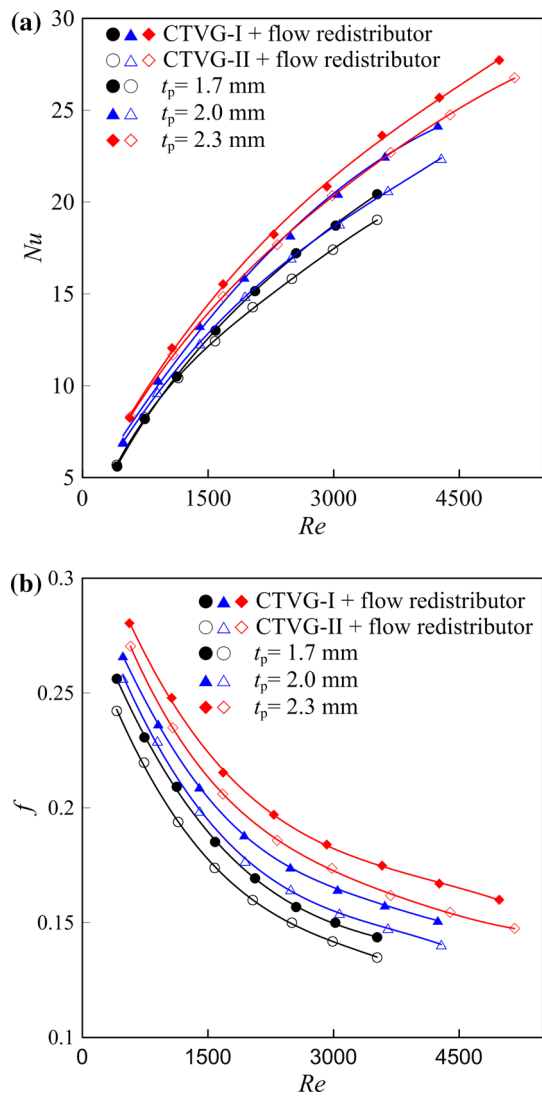
Fig. 11 Comparison of *Nu* and *f* between fins with VGs and flow redistributors: **a** *Nu*; **b** *f*

between fins with different fin pitches both increase with the increase of *Re* for both fin patterns. The value of *Nu* of the fin with CTVG-I and flow redistributors is larger than that of the fin with CTVG-II and flow redistributors. The difference in *Nu* between fins with CTVG-I and CTVG-II is very obvious and the difference increases with increasing *Re*. This is because CTVG-I which is larger than CTVG-II can generate stronger secondary flow and can induce more fluid to flow into the wake zone behind the tubes especially for large *Re*. *f* decreases with the increase of *Re* and increases with the increase of fin pitch for both fin patterns. The value of *f* of the fin with CTVG-I and flow redistributors is obviously larger than that of the fin with CTVG-II and flow redistributors.

From Fig. 11 we can find that the value of *Nu* of the fin with CTVG-I and $T_p = 2.0$ mm is nearly the same with

that of the fin with CTVG-II and $T_p = 2.3$ mm. Similarly, the value of *Nu* of the fin with CTVG-I and $T_p = 1.7$ mm is nearly the same with that of the fin with CTVG-II and $T_p = 2.0$ mm. The value of *f* of the fin with CTVG-I and $T_p = 1.7$ mm is obviously smaller than that of the fin with CTVG-II and $T_p = 2.0$ mm, and the value of *f* of the fin with CTVG-I and $T_p = 2.0$ mm is smaller than that of the fin with CTVG-II and $T_p = 2.3$ mm. Thus, the fin with both CTVG-I and flow redistributors has a better heat transfer performance than the fin with CTVG-II and flow redistributors.

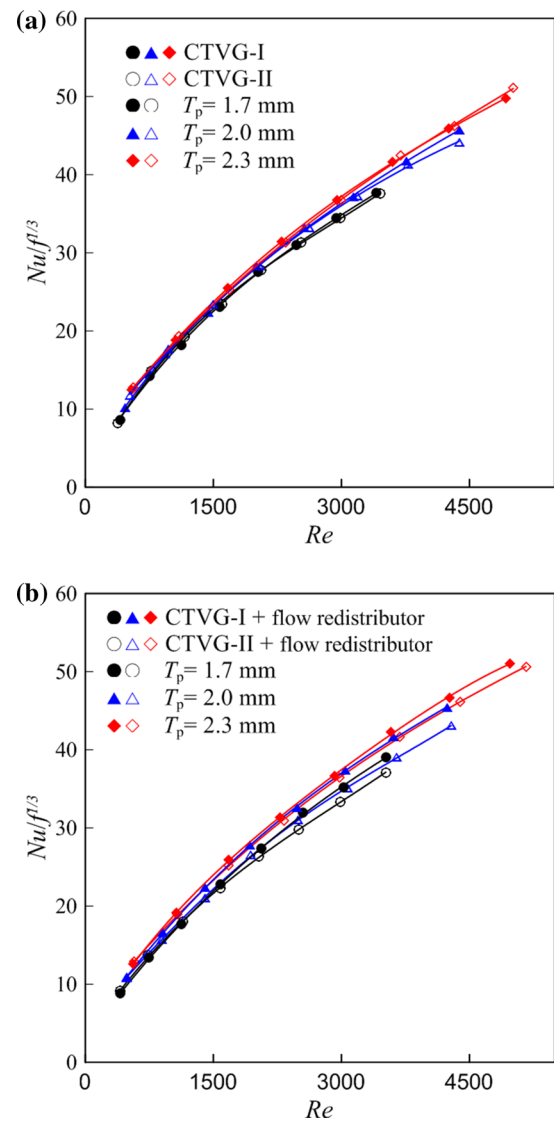### 4.5 Effects of flow redistributors on $Nu/f^{1/3}$

The heat transfer enhancement is always accompanied with the increase in pressure loss. The design goal of a new heat exchanger is to enhance heat transfer with lower pressure loss. $Nu/f^{1/3}$ can reflect the heat transfer performance based on the identical power. Figure 12a shows the effect of flow redistributors on $Nu/f^{1/3}$ of the plain fin. The value of $Nu/f^{1/3}$ increases with the increase of fin pitch for the plain fin. While for the plain fin with flow redistributors, the changing of fin pitch has a smaller effect on $Nu/f^{1/3}$ when $T_p > 1.7$ mm. From Fig. 6 we have known that flow redistributors located in front of the tube can decrease the friction factor at the cost of decreasing heat transfer for the plain fin when $T_p > 1.7$ mm, and the heat transfer is enhanced by flow redistributors when $T_p = 1.7$ mm. The value of $Nu/f^{1/3}$ of the plain fin with flow redistributors is the largest when $T_p = 1.7$ mm, and the values of $Nu/f^{1/3}$ are nearly the same when $T_p > 1.7$ mm. $Nu/f^{1/3}$ increases by 12.3% for the plain fin with $T_p = 1.7$ mm at $Re = 3690$. Figure 12b shows the effect of flow redistributors on $Nu/f^{1/3}$ for the fins with CTVG-I under different fin pitches. $Nu/f^{1/3}$ increases a little with the increase of fin pitch for both fin patterns. The value of $Nu/f^{1/3}$ increases due to the flow redistributors when $Re > 3000$, but the difference in $Nu/f^{1/3}$ between the fin with CTVG-I and the fin with CTVG-I and flow redistributors is very small. The values of $Nu/f^{1/3}$ are nearly the same when $Re < 3000$. $Nu/f^{1/3}$ of the fin with CTVG-I and flow redistributors is a little larger than that of the fin with CTVG-I when Re is larger than 3000. Figure 12c shows the distributions of $Nu/f^{1/3}$ for the fin with CTVG-II and the fin with CTVG-II and flow redistributors under different fin pitches. $Nu/f^{1/3}$ also increases a little with the increase of fin pitch for both fin patterns. But the value of $Nu/f^{1/3}$ of the fin with flow redistributors decreases due to the existence of flow redistributors, which is different from that of the fin with CTVG-I.

Figure 13a shows the comparison of $Nu/f^{1/3}$ of the fins with CTVG-I and CTVG-II under different fin pitches. $Nu/f^{1/3}$ increases slightly with the increase of fin pitch for both fins. The difference in $Nu/f^{1/3}$ between the fins with
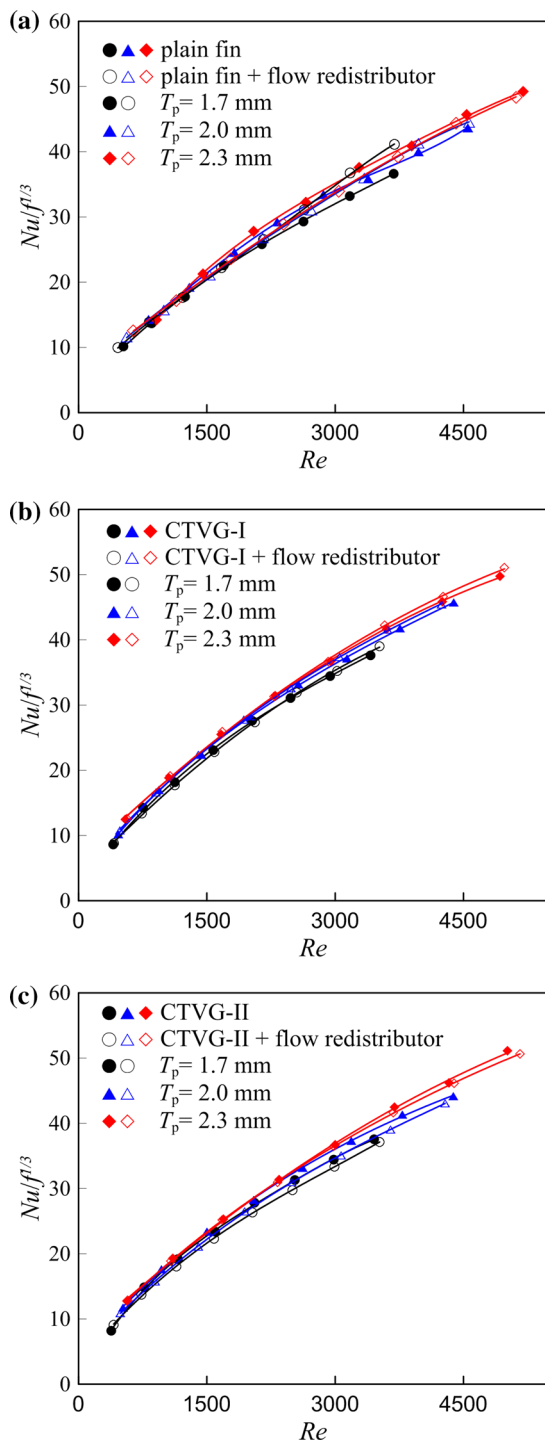
Fig. 12 Effect of flow redistributors on $Nu/f^{1/3}$ of different fin patterns: **a** plain fin; **b** CTVG-I; **c** CTVG-II

Fig. 13 Comparison of $Nu/f^{1/3}$ between the fins with CTVG-I and CTVG-II: **a** fins with CTVG; **b** fins with CTVG and redistributors

CTVG-I and CTVG-II is very small. The values of $Nu/f^{1/3}$ are nearly the same when $T_p = 1.7$ and 2.3 mm. The value of $Nu/f^{1/3}$ of the fin with CTVG-I is obviously larger than that of the fin with CTVG-II only when $Re > 3000$ and

$T_p = 2.0$ mm. $Nu/f^{1/3}$ increases by 3.6% when Re is about 4380.

The comparison of $Nu/f^{1/3}$ for the fins with flow redistributors and vortex generators is shown in Fig. 13b. The value of $Nu/f^{1/3}$ of the fin with CTVG-I and flow redistributors is larger than that of the fin with CTVG-II and flow redistributors. The difference in $Nu/f^{1/3}$ increases with the increase in Re. Compared to Fig. 13a, we can find that the difference in $Nu/f^{1/3}$ between the fins with CTVG-I and CTVG-II is obvious due to the existence of flow redistributors on the fin surface. The maximum value of $Nu/f^{1/3}$ of the fin with CTVG-I and flow redistributors increases by 5.2, 5.5 and 2.6% for $T_p = 1.7$, 2.0 and 2.3 mm, respectively.

5 Conclusions

The effect of flow redistributors stamped out from the fin surface in front of the stagnation points of tubes on the air-side performance of tube-fin heat exchanger is experimentally studied for both the plain fin and the fin with curved triangular vortex generators under different fin pitches. Two sizes of curved triangular vortex generators are considered. The main conclusions are drawn as follows.

(1) The flow redistributors can decrease the values of both f and Nu for the plain fin. The existence of flow redistributors can decrease f at the cost of decreasing Nu for the plain fin. The value of $Nu/f^{1/3}$ is slightly affected by flow redistributors when the fin pitch is greater than 1.7 mm. The maximum value of $Nu/f^{1/3}$ increases by 12.3% due to the flow redistributors for the plain fin with $T_p = 1.7$ mm.

(2) CTVG-I can enhance the value of Nu effectively at the cost of increasing the friction factor. But for the fin with CTVG-II, the existence of flow redistributors decreases the value of Nu and increases the value of f.

(3) The values of Nu and f of the fin with CTVG-I are larger than those of the fin with CTVG-II, and the difference in Nu between fins with CTVG-I and CTVG-II increases due to the existence of flow redistributors, but the friction factor changes a little.

(4) $Nu/f^{1/3}$ for the fin with CTVG-I and flow redistributors is obviously larger than that of the fin with CTVG-II and flow redistributors. The maximum value of $Nu/f^{1/3}$ increases by 5.2, 5.5 and 2.6% for $T_p = 1.7$, 2.0 and 2.3 mm, respectively.

References

1. Wang CC, Liaw JS, Yang BC (2011) Airside performance of herringbone wavy fin-and-tube heat exchangers data with larger diameter tube. Int J Heat Mass Transf 54:1024–1029
2. Yun R, Kim YB, Kim YC (2009) Air side heat transfer characteristics of plate finned tube heat exchangers with slit fin configuration under wet conditions. Appl Therm Eng 29:3014–3020
3. Phan TL, Chang KS, Kwon YC, Kwon JT (2011) Experimental study on heat and mass transfer characteristics of louvered fin-tube heat exchangers under wet condition. Int Commun Heat Mass Transf 38:893–899
4. Joardar A, Jacobi AM (2008) Heat transfer enhancement by winglet-type vortex generator arrays in compact plain-fin-and-tube heat exchangers. Int J Refrig 311:87–97
5. Huisseune H, T'Joen C, Jaeger PD, Ameel B, Schampheleire SD, Paepe MD (2013) Performance enhancement of a louvered fin heat exchanger by using delta winglet vortex generators. Int J Heat Mass Transf 56:475–487
6. Tian LT, He YL, Tao YB, Tao WQ (2009) A comparative study on the air-side performance of wavy fin-and-tube heat exchanger with punched delta winglets in staggered and in-line arrangements. Int J Therm Sci 48:1765–1776
7. Tang LH, Zeng M, Wang QW (2009) Experimental and numerical investigation on air-side performance of fin-and-tube heat exchangers with various fin patterns. Exp Therm Fluid Sci 33(5):818–827
8. Tang LH, Xie GN, Zeng M, Lin M, Wang QW (2008) A comparative study of fin-and-tube heat exchangers with various fin patterns. In: ASME conference proceedings of the Heat Transfer Part A and B, 4, pp 1239–1246
9. Tang LH, Zeng M, Xie GN, Wang QW (2009) Fin pattern effect on air-side heat transfer and friction characteristics of fin-and-tube heat exchangers with large number of large-diameter tube rows. Heat Transf Eng 30:171–180
10. Zeng M, Tang LH, Lin M, Wang QW (2010) Optimization of heat exchangers with vortex generator fin by Taguchi method. Appl Therm Eng 30:1775–1783
11. Wu JM, Tao WQ (2008) Numerical study on laminar convection heat transfer in a channel with longitudinal vortex generator part B: parametric study of major influences factors. Int J Heat Mass Transf 51:3683–3692
12. Song KW, Wang LB, Fan JF, Zhang YH, Liu S (2008) Numerical study of heat transfer enhancement of finned flat tube bank fin with vortex generators mounted on both surface of the fin. Heat Mass Transf 44(8):959–967
13. Gao SD, Wang LB, Zhang YH, Ke F (2003) The optimum height of winglet vortex generators mounted on three-row flat tube bank fin. J Heat Transf 125:1007–1016
14. Liu S, Wang LB, Fan JF, Zhang YH, Song KW (2008) Tube transverse pitch effect on heat/mass transfer characteristics of flat tube bank fin mounted with vortex generators. J Heat Transf 130:1–3
15. Song KW, Wang LB (2016) Effects of longitudinal vortex interaction on periodically developed flow and heat transfer of fin-and-tube heat exchanger. Int J Therm Sci 109:206–216
16. Zhang YH, Wang LB, Ke F, Su YX, Gao SD (2004) The effects of span position of winglet vortex generator on local heat/mass transfer over a three-row flat tube bank fin. Heat Mass Transf 40:881–891
17. Hu WL, Su M, Wang LC, Zhang Q, Chang LM, Liu S, Wang LB (2013) The optimum fin spacing of circle tube bank fin heat exchanger with vortex generators under the same front velocity. Heat Mass Transf 49:1271–1285
18. Jang JY, Hsu LF, Leu JS (2013) Optimization of the span angle and location of vortex generators in a plate and tube heat exchanger. Int J Heat Mass Transf 67:432–444
19. Song KW, Xi ZP, Su M, Wang LC, Wu X, Wang LB (2017) Effect of geometric size of curved delta winglet vortex generators and tube pitch on heat transfer characteristics of fin-tube heat exchanger. Exp Therm Fluid Sci 82:8–18
20. Lotfi B, Sundén B, Wang QW (2016) An investigation of the thermo-hydraulic performance of the smooth wavy fin-and-elliptical tube heat exchangers utilizing new type vortex generators. Appl Energy 162:1282–1302
21. Colleoni A, Toutant A, Olalde G, Foucaut JM (2013) Optimization of winglet vortex generators combined with riblets for wall/fluid heat exchange enhancement. Appl Therm Eng 50:1092–1100
22. Zhou GB, Feng ZZ (2014) Experimental investigations of heat transfer enhancement by plane and curved winglet type vortex generators with punched holes. Int J Therm Sci 78:26–35
23. Qian SW (2002) Handbook of heat exchanger design. Chemical Industry Press, Beijing
24. Narayanan CM, Bhattacharya BC (2007) Unit operations and unit processes, vol 1. CBS Publishers, New Delhi
25. Schmidt TE (1949) Heat transfer calculation for extend surface. Refrig Eng 57:351–357

26. Gray DL, Webb RL (1986) Heat transfer and friction correlations for plate fin-and-tube heat exchangers having plain fins. In: 8th international heat transfer conference, San Francisco, California, pp 2745–2750

27. Wang CC, Chang YJ, Hsieh YC, Lin YT (1996) Sensible heat and friction characteristics of plate fin-and-tube heat exchangers having plain fins. Int J Refrig 19:223–230

28. Moffat RJ (1982) Contribution to the theory of single-sample uncertainty analysis. ASME J Heat Transf 104:250–260

29. Song KW, Wang LB (2013) The effectiveness of secondary flow produced by vortex generators mounted on both surfaces of the fin to enhance heat transfer in a flat tube bank fin heat exchanger. ASME J Heat Transf 135(4):041902

30. Song KW, Hu WL, Liu S, Wang LB (2016) Quantitative relationship between secondary flow intensity and heat transfer intensity in flat-tube-and-fin air heat exchanger with vortex generators. Appl Therm Eng 103:1064–1070

31. Song KW, Liu S, Wang LB (2016) Interaction of counter rotating longitudinal vortices and the effect on fluid flow and heat transfer. Int J Heat Mass Transf 93:349–360

32. Hu WL, Song KW, Guan Y, Chang LM, Liu S, Wang LB (2013) Secondary flow intensity determines Nusselt number on the fin surfaces of circle tube bank fin heat exchanger. Int J Heat Mass Transf 62:620–631